UNIVERSITY of NEW HAMPSHIRE

Tech 797 | 2011-2012

Cohesive Incipient Motion

Ben Anibal
Laura Baldinger
Dustin Metayer

Faculty Advisor: Dr. Diane Foster

Mechanical Engineering and Ocean Engineering Departments of the University of New Hampshire

Table of Contents

Objectives

Camera analysis is being performed to examine the incipient motion of sand particles at the base of a circular wave flume in Gregg Hall at the University of New Hampshire in Durham, New Hampshire. Images of particle motion are being captured with Point Grey's high-resolution CCD camera, the Grasshopper 2. Once the images are collected, they are analyzed in a Matlab program, MatPIV, which determines their velocity vectors and velocity, knowing the times the images were captured. The objective of this yearlong project is to learn proper technique for sediment transport analysis. This technique could be used in imperative situations, such as oil spills, where it needs to be determined if oil particles are moving or not to initiate the most effective cleanup protocol.

To validate this camera analysis technique before the main objective is accomplished, a dry run of the experiment using the same camera analysis procedure will be performed. A sand-bed will be constructed and pulled using a pulley system across a table surface. The Grasshopper 2 will capture the particle images to be analyzed in MatPIV. The velocities obtained in the Matlab program will be compared to experimentally collected velocities found using kinematic equations. Distance and timing of the sand-bed in motion will be collected to use in the kinematic equations. If the MatPIV program provides the same velocities as the experimentally derived velocities via the kinematic equations, it can be concluded that this MatPIV camera analysis technique is valid.

Before measurements are taken in the circular wave flume in Gregg Hall, a specific position in the tank must be chosen based off of velocity measurements. A site with uniform flow is desired. Velocity measurements will be taken with Nortek's 3D velocimetry sensor, the Vector. Once a position has been chosen, data for a 3D flow map will be collected.

Based on the collected velocity measurements, a sediment size will be chosen to enable incipient motion of sediment at the base of the flume to be captured using the camera. Once captured, the particles images will be analyzed in MatPIV.

Theory and Experimental Methods

I. Incipient Motion

Incipient motion can be thought of as the single moment in time when a particle begins to move from rest. The determination of this time depends on many factors, including both the particle(s) in question and the surrounding flow. Attempts at models to develop formulae for incipient motion have been made, but presently dimensional analysis is the only accepted method in determining the most likely time in which incipient motion will begin. One of the first to work with developing relations for incipient motion was Albert F. Shields, who in 1936 defined what is known as the Shields parameter. Today, the Shields parameter is still accepted in the study of sediment transport. This parameter, defined as a dimensionless shear stress, holds as the critical parameter to define the start of particle movement.

Before looking closely at the parameters and Shields diagram, the forces on an individual grain in the sand bed can be balanced. Below is the free body diagram displaying all relevant forces acting on the particle, assuming it is resting on a bed of more sand grains. The force of gravity acts downward, lift acts upward, drag acts in the direction of the flow, and there is a resistive force up and against flow from the particle below.

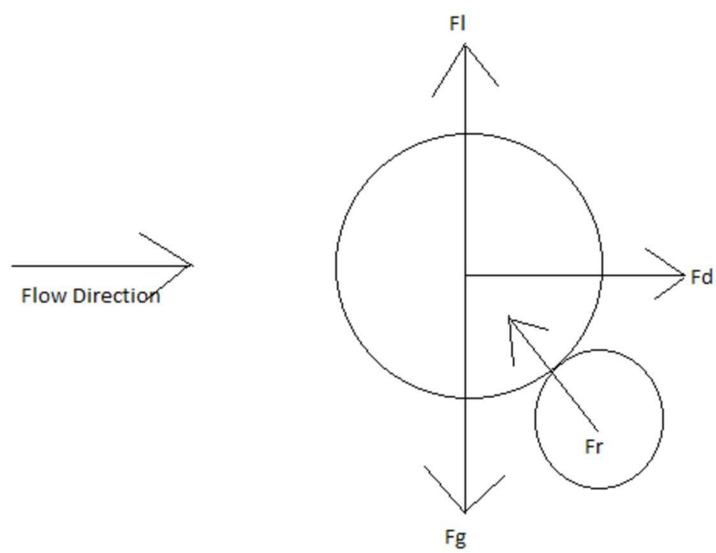

Figure 1: Force balance on bed particle.

Using a force balance, two equations can be made for the x and y directions, assuming a time before the advent of motion. These being:

$$F_L + F_g + F_R Y = 0 \quad and \;\; F_D + F_R X = 0 \tag{1}$$

The force of gravity for a submerged particle is related to its volume and density with:

$$F_g = \left(\rho_{sediment} - \rho_{H_2O}\right) \cdot gravity \cdot \left(\frac{\pi}{6} \cdot D_{grain}^3\right) \tag{2}$$

The lift force on the particle is found using the velocity of the flow at the top and bottom of the particle, U_T and U_B, respectively, along with the coefficient of lift, c_L, which is roughly 0.2 for a sphere. Area is defined as the cross sectional area perpendicular to flow.

$$F_L = \rho \cdot \left(\frac{C_L}{2}\right) \cdot (U_T^2 - U_B^2) \cdot Area \tag{3}$$

Drag force is found in a similar manner with the use of a flow field, U, speed assuming the particle was not there.

$$F_D = \rho \cdot \left(\frac{C_D}{2}\right) \cdot U^2 \cdot Area \tag{4}$$

With the use of a logarithmic flow profile near the bed floor, and the " Von Karman coefficient", roughly .41, the drag force will become:

$$F_D = \tau_b \cdot \frac{C_D}{2} \cdot F^2 \cdot \left(\frac{D}{Z_o}\right) \cdot Area \tag{5}$$

where

$F^2 \cdot \left(\frac{D}{Z_o}\right) = \left[\frac{1}{k} \cdot \ln\left(\frac{D}{Z_0}\right) - 1\right]^2 \quad D = particle\ diameter \quad Z_0 = bed\ location\ of\ zero\ velocity$

The above equation uses the Von Karman coefficient, k, to describe the velocity at the bed of a turbulent flow, assuming a no slip condition. This flow field is described as:

$$u(z) = \frac{u_*}{K} \cdot \ln\left(\frac{z}{z_o}\right) \tag{6}$$

where

$u_* is\ a\ velcoity\ scale\ to\ characterize\ the\ boundry\ layer$

The resistive force can be broken into x and y components, and the critical drag force set equal to the x component of the resistive force. Relating all previous forces, and setting the bed stress equal to the density of the particle times the characteristic velocity squared, the equation becomes:

$$\frac{\tau_{bcrit}}{\rho \cdot (s-1) g \cdot D_s} = \frac{4 \cdot \tan(\phi)}{3F^2\left(\frac{D}{Z_0}\right)\left(1 + \frac{F_L}{F_d} \cdot \tan(\phi)\right)} = \frac{u_*^2}{(s-1)g} \cdot D_s = \theta = Shields\ Parameter \tag{7}$$

This is the Shields parameter, which is roughly a relation of drag force over the immersed weight of the particle. The critical Shields parameter defines the beginning of motion and requires the knowledge of the critical velocity, or critical bed stress. In order to calculate the critical bed stress, a particle Reynolds number can be defined to directly plot against critical bed stress. The particle Reynolds number is a dimensionless number defined as:

$$R_p = \frac{\sqrt{RgD}D}{\nu} \tag{8}$$

where

$R = \dfrac{\rho_s - \rho}{\rho}\ and\ D = median\ grain\ size$

With this number, a fit to Shields data and the critical bed stress was given by Brownlie as:

$$\tau_c^* = 0.22 R_p^{-0.6} + .06\mathrm{e}^{-17.77\mathrm{R_p}^{-0.6}} \tag{9}$$

The figure below shows various data plotted on the curve that relates the Reynolds particle number to critical bed stress. Knowing simple flow characteristics and particle information leads to the discovery of a theoretical bed stress; this can then be used to determine the speed at which incipient motion will begin. It should be note that this is not the original Shields curve, which relates the particle Reynolds number to shear stress directly.

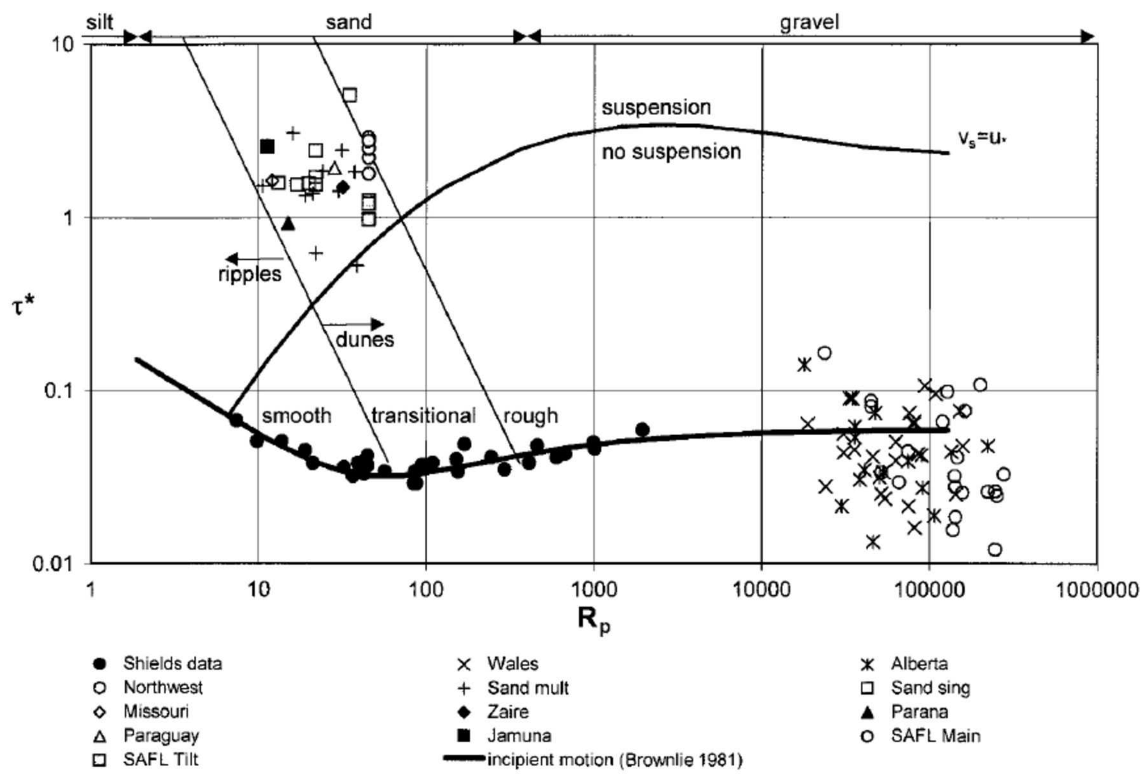

Figure 2: Shields diagram plotted with additional data and Brownlie equation

This curve allows for a comparison between mostly sand beds and mostly gravel beds. The large set of data located to the lower right is for gravel-bed rivers. Here, the maximum shear stress is only twice the critical shear stress for transport, and sediment transport requires nearly full flow. For sand beds, as seen in the test data in the upper left, shear stress was 20 to over 60 times that needed for incipient motion. This leads to more constant sediment transport, which often occurs in suspension, as seen by the dividing upper line.

Use of this curve can be helpful in determining sizing needs for a study. Between a model and prototype parameters, both should have the same particle Reynolds number and the same Shields stress. Further use of the curve can help to predict flow speeds that will be needed to begin the onset of incipient motion. The previous analysis neglects unsteady flows and focuses only on invariant unidirectional flow. Waves in the flow, along with any underwater pressure gradients, were also ignored due to their variability and difficultly in modeling for a wide range of conditions.

II. Camera

The camera selected for this project was chosen based off the need for a field of view of about 15 centimeters by 15 centimeters to resolve sand grain sizes with a diameter of 5 centimeters. It was also chosen based off of the criterion to capture image frames at 30 Hz or frames per second. The company Point Grey was recommended by Tom Lippman of CCOM.

Point Grey's Grasshopper 2 was chosen as it fit the desired criteria, pictured in Figure 3. The Grasshopper 2 is very compact, 58 mm x 44 mm x 29 mm, which is beneficial for a flow analysis where reduced flow disturbance is preferred. It has a maximum resolution of 1384 by 1036 pixels, with a pixel size of 6.45 by 6.45 micrometers. It has a maximum frame rate of 30 frames per second at this maximum resolution, 1384 x 1036.

Figure 3: Point Grey's Grasshopper 2

The Grasshopper 2 has dual 9-pin IEEE-1394b 800 Mb/s ports interface. This interface allows the camera to be directly connected to a computer via a FireWire cable. An 800 Mb/s 9-pin to 6-pin FireWire cable was used to connect the Grasshopper 2 to a MacBook with a 6-pin FireWire Port.

The specification sheet for this camera can be found in the appendices.

III. Camera Analysis: MatPIV

Particle Image Velocimetry, PIV, image analysis was used as the method to determine the velocity of particles along the sand bed. A basic PIV study yields the instantaneous two dimensional velocity vectors for a given area of flow, which can be used to create a real time mapping of velocities at a point over a set period of time. The use of multiple offset cameras (stereoscopic arrangement) can be used to find the 3D flow of particles, although this was not used in this project and vertical flow was not accounted for.

The methods for velocity calculation, as utilized by MatPIV and other PIV software, look at the relative change in distance among particles for a given time period. The use of a steady light or a synchronized strobe illuminates the particles at each camera image. Subsequent pairs of images are further divided into interrogation areas (IA), and the pixels of each IA are compared between the two images. Correlations between consecutive IA's at the same spatial location identify the average particle displacement for that area. A velocity map for the entire field can be calculated by finding correlations among all IA's. An important factor to ensure accurate calculations is to set the interrogation window size such that on the order of 10-20 particles are seen. Any particles that travel out of the interrogation window during a time step will also result in a loss of correlation. To combat this, the change in distance travelled should be on the order of 25% of the change in the length of the interrogation window.

MatPIV, a free software toolbox for Matlab, was used to create the code that calculates the velocity vectors of the flow field. The options available and the filters provided allow for a wide variety of analyses, but a set of basic options must be used for all trials. The captured frame rate, either 15 Hz or 30 Hz, for sediment transport initializes the time step. The interrogation window, in pixels, must be set following the previously stated principles. Using a single pass over the interrogation window, the program will output four matrices, the x any y coordinates in pixels and the u and v velocities in pixels per second. In order to calculate real world velocities, a scale image must be taken and the pixels/cm conversion is used to find a speed in meters/sec. Results can be filtered using a signal to noise ratio, which eliminates erroneous vectors due to particle saturation or insufficient matching between images. Analysis between a pair of images can be visualized with a velocity vector map. In this project an iterative loop was used to find the velocity at a single point for a series of many images over a longer period of time.

IV. Dry Experiment: CCD Camera Measurement of Ogunquit Sand Velocity

A dry experiment was performed prior to any in water testing to validate the MatPIV camera analysis technique. Particle images were collected using the Grasshopper 2 and then analyzed in Matlab.

The test structure used to calculate incipient velocity of sand from Ogunquit, Maine consists of a 24" by 12" piece of pinewood plywood surrounded on both sides by cardboard of the same size. Before the pieces were glued together, a hole was drilled in the center of one end of the plywood and a 100 lb. fishing line was tied to the hole. Two 12" long, 1" angle irons were glued on top of the top layer of cardboard to simulate ripples, seen in Figure 4.

Figure 4: Sand bed test structure

The sand was attached to the top of the sand bed test structure using spray adhesive. The test structure was placed on top of a wooden laminated tabletop. The fishing line attached to the test structure was attached to a 1.5-pound mass on the opposite end. The fishing line ran over a pulley attached to the end of the table. When the mass was released at the end of the table, the test structure slid across the table.

The static coefficient of friction between the tabletop and the bottom cardboard piece of the test structure was calculated using Equation 10. The static coefficient of friction between two solid surfaces is equal to the tangential force required to produce sliding divided by the normal force between the surfaces.

$$\mu = \frac{F}{N} \tag{10}$$

where
μ is the static coefficient of friction
F is the tangential force
N is the normal force

In this scenario, the tangential force is the weight of the dropped mass and the normal force is the weight of the sand bed test structure.

The velocity of a single grain of sand was calculated using MatPIV and Dantec Flow Manager. Individual images were collected using Point Grey's Grasshopper high resolution CCD camera using the software program Astro IIDC. The camera was setup on a tripod facing downwards capturing the sand particles as the test structure slid across the tabletop. This setup can be seen below in Figure 5.

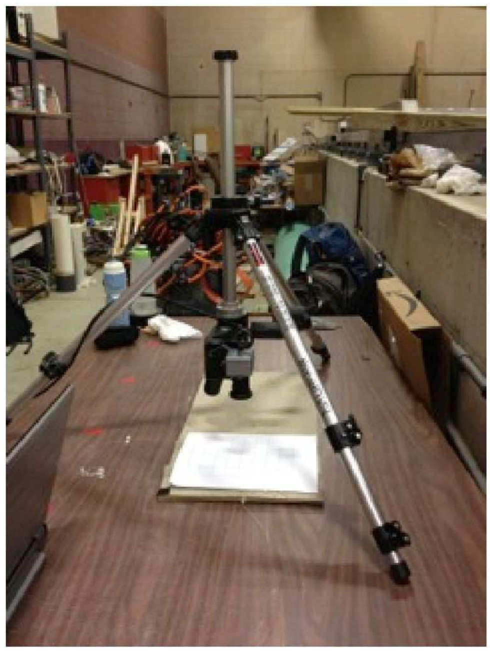

Figure 5: Camera and sand bed test structure set up

The velocity calculated using the velocity vectors in the MatPIV program was compared to the velocity of the sand bed calculated using the law of conservation of energy equation and the kinematic equations of motion.

The conservation of energy equation equates potential energy to kinetic energy.

$$PE = KE$$

$$m_1 gh = \frac{1}{2} m_2 v^2 \tag{11}$$

where
m_1 is the mass of the potential energy contributor
g is gravity
h is the height of m_2
m_2 is the mass of the kinetic energy contributor
v is the velocity of m_2

For this procedure, m_1 is the mass of the weights being dropped at the end of the table and h is the height of the table. The mass of the sand bed test structure is m_2 and the velocity of the test structure is the unknown being calculated. Rearranging the conservation of energy equation, Equation 12, shows how the velocity of the sand bed was computed.

$$v = \sqrt{\frac{2 \cdot m_1 \cdot g \cdot h}{m_2}} \tag{12}$$

This velocity was verified with the velocity of the sand bed test structure calculated using the kinematic equations of motion. Equation 13 takes the initial, final velocity and the time elapsed over a defined distance into account.

$$d = \frac{v_i + v_f}{2} \cdot t \tag{13}$$

where
d is the distance traveled
v_i is the initial velocity
v_f is the final velocity
t is the time elapsed

In Equation 13, the final velocity represents the velocity of the sand bed test structure to be solved for. The initial motion of the sand bed is zero. The time elapsed was captured using a stopwatch and the distance was measured using a tape measure. Rearranging Equation 13, the sand bed test structure velocity was calculated using the following equation.

$$v_f = \frac{2 \cdot d}{t} - v_i \tag{14}$$

V. Tank Construction

The circular tank was assembled by Charlie Watkins, a Civil Engineering student at the University of New Hampshire, and by Nick Tamblyn. Since the end goal of this experiment is to put oil in the tank to collect incipient motion data of oil sediments, the subfloor of the tank was designed with these intentions in mind. The subfloor was mandated by the town of Durham, New Hampshire to ensure entrapment of the oil-water mixture in the volume. A sidewall was constructed with a liner to hold 600 gallons of fluid as a precautionary for any leaks. The tank has a maximum capacity of 4000 liters of fluid but the tank is limited to a volume of 2000 liters due to the limitations of the university. The tank consists of 4 large outer radius sections and 3 inner radius sections.

The tank outer diameter is 11 feet with a 7 foot inner diameter. This provides a usable fluid cross section of 2 feet and ¾ inches. There is a 5 inch height difference between the inner and outer sections of the tank. This is because previously the tank contained a weather vain to generate waves inside the tank. The tank contains an additional prevention measure to prevent its inability to seal the gaps between the Lexan and the aluminum tank structure.

VI. Flow Straightener

Researching was imperative in understanding how to properly straighten the flow in the circular tank in Gregg Hall. The principle behind a flow straightener is to insert an object to sub-divide a large-scale turbulent flow that is spread out across the tank cross-section. The flow straightener uses smaller cross-sectional tubes or channels to sub-divide the large scale circular flow. As the flow passes through the flow straightener the flow becomes fully developed in the smaller section tubes or channels. The small sections of fully developed flow create a uniform flow on the exiting side of the flow straightener. When the flow reunites on the exiting side of the flow straightener, uniform flow is established. The reduction of turbulence depends on the length of the flow straightener and the cross-sectional area of the individual tube or channel. The smaller the cross-sectional areas of the individual tube or channel are, the smaller the turbulence. The length of the flow straightener enables the flow to fully develop. This depends on the viscous effects, the velocity of the fluid, and the density of the fluid.

The selection of the length of the flow straightener was decided from research and a scale comparison from previous masters' theses on the development of a water tunnel. An additional safety factor to guarantee fully developed flow. The masters' theses of John Rule and Christopher Doane were used to select the length of the flow straightener. The flow straightener developed for both Doane and Rule's tanks had an overall length of 1 foot of PVC pipe. Rule embedded the pipes into the concrete of the flume. The circular tank's geometry is inconsistent in comparison to both of the master theses flumes as the theses provided data for an oval flume with straight test sections. For this project, the circular tank in Gregg Hall at University of New Hampshire is being used, which is comprised of two cylindrical inner and outer tank sections. Due to different geometries of the flumes an additional length to the straightener was added to allow the flow to become fully developed inside the flow straightener tubes or channels. A safety factor of 1.5 was chosen to multiply by the selected length previously used in Rule and Doane's theses, making the length of the flow straightener 16 inches.

Figure 6: Final construction of the flow straightener

The volume of the flow straightener was selected to be 16 inches by the tank diameter by a foot and a half of tank height. The material selection was chosen to resemble honeycomb, which is used to straighten flow for some wind and water tunnels. The selected material was a clear polycarbonate corrugated roofing panel. These panels were stacked together to create a hexagon pattern for a flow straightener cross-sectional area. A template was attached and traced onto the material from a predesigned template prior to stacking the material. A template consisting of arcs on the ends the material created by using a string and a pivot point. A pivot point at the radius of the inner and outer sections of the tank and a pen to mark the arcs on a cardboard template were used. The radii were marked out onto the material, and then the pattern was cut using sheet metal tin-snips. The corrugated panels were stacked and held together using aluminum 1/8-inch grip by 1/8-inch depth rivets. The aluminum rivets allow for a rust free flow straightener, in case salt water was to be used in future experiments. The patterns were cut to the precise dimensions of inner and outer radius of the tank to allow for the straightener to slide right into position in the tank with no braces to hold the flow straightener. Braces would interrupt the flow causing turbulent vortices.

VII. Instrumentation

As mentioned above, the Grasshopper 2 camera is one of the instruments being used to collect velocity data. The other devices used to collect velocity are velocimetry sensor instruments. The velocimetry sensors, belonging to Dr. Diane Foster, are Nortek's Vector, Vectrino II, and Aquadopp.

The Vector was used in this experiment to collect velocity measurements at various positions in the wave flume. The Vector is a high-resolution acoustic velocimetry instrument used to measure 3D water velocity, pictured in Figures 7 and 8.

Figure 7: Nortek's Vector

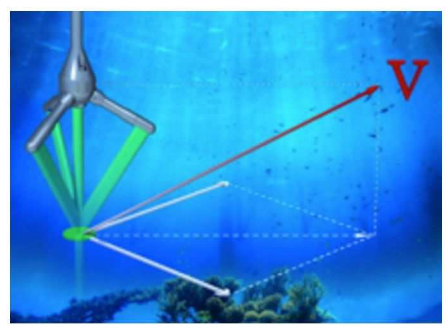

Figure 8: 3 velocity components of the Vector

The Vector collects velocity data using coherent Doppler processing, seen in Figure 8. It collects data using three velocity components, one in the x-direction, y-direction, and z-direction to obtain 3D velocity results. The Vector has the ability to collect temperature, pressure, tilt, and compass readings along with velocity readings. In this experiment, only the velocity measurements are being recorded.

Its sampling volume is 0.15 meters from the probe, at a diameter of 15 millimeters and a height ranging from 5-20 millimeters. It can sample at an output of a range from 1 to 64 Hertz. The specification sheets for the Vector and data tables of collected data are located in the appendices.

For more precise velocity measurements for this scale of an experiment, it is advised the Vectrino II be used to collect additional velocity data. The Vectrino II similarly measures 3D velocity but at rates up to 100 Hertz, faster than the Vector's maximum frequency of 64 Hertz. It also has a vertical range of 3 centimeters, with a resolution of 1 millimeter.

Due to time constraints, only the Vector was used to collect data. The Vectrino II and Aquadopp should be used in the tank to collect additional velocity readings for comparison purposes.

The Nortek instruments come with a complete suite of Windows 2000/XP software for data collection. Figure 9 shows the Vector II being used for data collection in the tank.

Figure 9: Vector being used to collect velocity measurements in the tank

VIII. Instrument Mounts

The motor mount was designed to preserve the integrity of the tank liner's high density plastic. The motor mount was designed to simulate the natural usage of the current stage transom mount trolling motor. The mount maintains the integrity of the tank by using additional 2 inch by 2 inch 90 degree aluminum, which is lowered down the sidewalls of the tank. The 2 inch by 2 inch 90 degree aluminum angle iron supports a 2 inch by 6 inch pine board, which spans the cross-section of the tank. All of the components are held together with stainless steel 5/16 inch bolts and nuts.

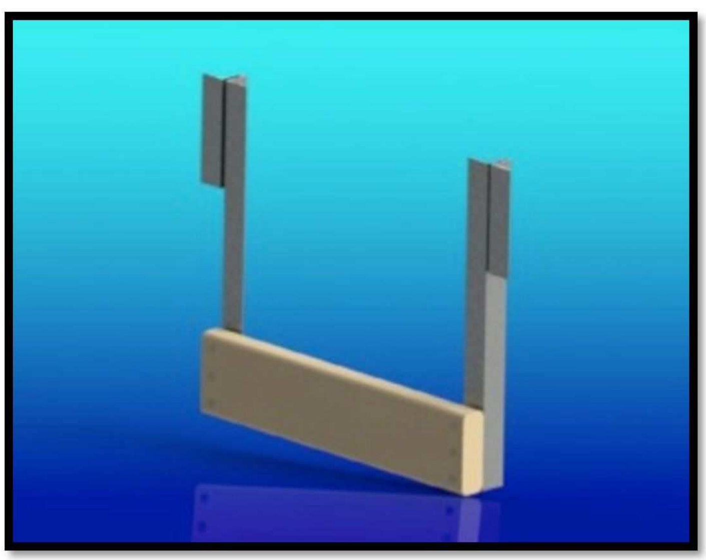

Figure 10: Design of the trolling motor's mount in SolidWorks

The trolling motor mount was designed to hold the maximum thrust of the trolling motor at the maximum depth. The trolling motor mount was designed to withstand 225 ft-lbs of torque at the center point of the beam or transom. The design calls for the mount to be bolted to the upper rim of the tank for a secure connection point, so any failure of the connection point would be from shear of the stainless steel bolts rather than failure of pure clamping between material sections.

The camera mount was designed very similarly to the trolling motor mount. The only difference was using different angle iron since this mount will not experience nearly as much torque as the trolling motor mount. 1 inch by 1 inch, 90 degree aluminum angle iron was used instead of the 2 inch by 2 inch, 90 degree aluminum angle iron.

Figure 11: Camera pressure case and mount

Figure 12: Camera pressure case, mount, and flow straightener

The camera mount can be seen in Figures 11 and 12. It should also be noted that a pressure case had to be constructed to hold the camera and keep it dry. The pressure case consists of a 3-inch diameter gray PVC pipe. An end cap with a 2.5-inch diameter hole was placed on the end of the gray PVC pipe. A piece of Lexan was cut to place between the end cap and the pipe, creating a lens. The components were glued together using JB weld to create a watertight seal.

The pressure case was held to the mount using two 2 inch to 3 inch diameter pipe clamps and another piece of 1 inch by 1 inch, 90 degree aluminum angle iron. The angle iron was screwed to the plywood using two 5/16 inch bolts and nuts.

When looking back at Figure 9, it can be seen that the camera mount was suitable for the Vector as well.

Results and Discussion

I. Dry Experiment: CCD Camera Measurement of Ogunquit Sand Velocity

Tables 1 and 2 show the results of the dry experiment discussed previously. These tables represent the velocities found using the kinematic equations. The particle imagery data sought to be collected was unreliable. The MatPIV program could not decipher the velocities due to too much blur of the sequential images. The velocity vectors went haywire so modifications had to be made to this experiment to acquire reliable data to validate this camera analysis method.

Table 1: Raw data collected from the estimation of the velocities, using a constant mass system

Test	Time (2'-2") (sec)	Distance Traveled, Sand Bed (inches)	Distance of dropped Mass (inches)
1	1.46	36	26
2	1.48	36	26
3	1.13	36	26
4	1.59	35	26
5	1.59	34	26

Table 2: Kinematic equations of motion results using the time between a known to distinct points

	Kinematic Equations of Motion		$d = (v_i + v_f)/2 * t$	
Test	Time (2'-2") (sec)	Distance Traveled, Sand Bed (inches)	Final Velocity (in/sec)	Final Velocity (ft/sec)
1	1.46	36	2.47E+01	2.05E+00
2	1.48	36	2.43E+01	2.03E+00
3	1.13	36	3.19E+01	2.65E+00
4	1.59	35	2.20E+01	1.83E+00
5	1.59	34	2.14E+01	1.78E+00

As you can see above, the velocity measurements ranged from 1.8 ft/sec to 2.7 ft/sec. These velocities are much too fast for the camera to capture clearly to perform this analysis. The main modification made to this experiment was putting a lesser weight on the end of the pulley to slide the sand test structure, which slowed the velocity down. Also, light was added to the experimental set-up to reduce blur.

The experiment was performed again with these modifications and the velocities were able to be resolved in MatPIV. No reference frame was captured to determine the magnitude of the velocities, but the MatPIV program showed the velocity vectors aligned well with the direction of motion of the sliding test structure, so it was concluded that this camera analysis technique was valid.

II. Tank Construction

The overall tank construction is set to the town of Durham's environmental standards according to Charlie Watkins. The tank provides poor flow properties due to the tank's liner and the orientation of a circular tank. The tank liner has ridges from excess material, which creates vortices in the downstream flow, as well as high flow gradients perpendicular to the mean flow direction. For improvement, it is recommended that the material ridges be reduced in the tank either by tightening the liner or by removing the liner all together from the tank. Sealing the tank with a longer cure time silicone caulk, which perhaps allows the caulk to settle into the nooks and crannies of the tank gaps and rids the tank of the mentioned unwanted flow characteristics.

III. Flow Field Velocity Measurements

As previously discussed, velocity measurements were collected using the Vector. 8 angles were chosen around the circular wave flume, shown in Figure 13. First, 3D velocity measurements were collected at these 8 angles in the middle of the board, notation shown in Figure 14. In Figure 14, position 1 is in the middle of the board. Positions 2 and 5 are located 6.5 inches away from the tank wall. Position 2 is 6.5 inches away from the outer wall of the tank and position 5 is 6.5 inches away from the inner wall of the tank. Positions 3 and 4 are 9 inches away from the outer wall and inner wall of the tank, respectively.

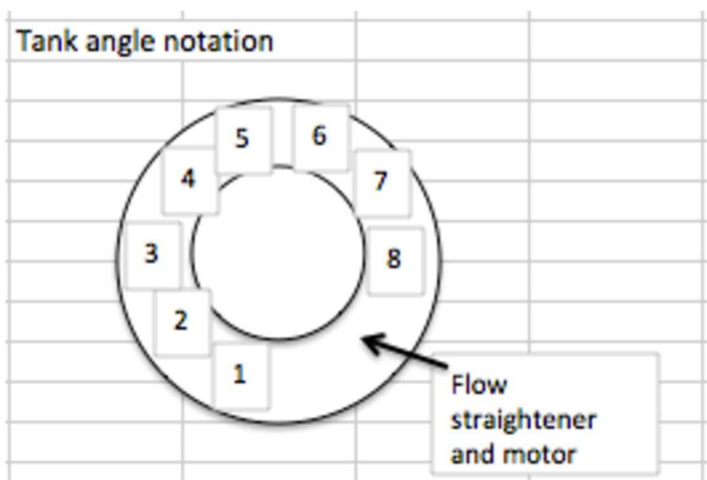

Figure 13: Tank angle notation for Vector velocity measurements

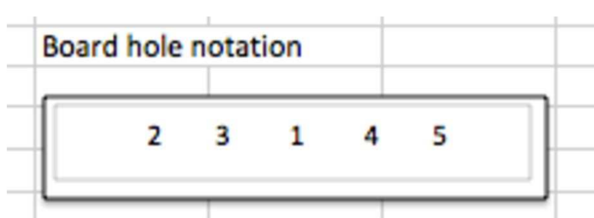

Figure 14: Board hole notation for Vector velocity measurements

The first round of measurements to choose the location were taken when the probe was 10 centimeters away from the base. This was later resolved to be an inaccurate set of measurements, as the sample volume requires the probe to be at least 15 centimeters away from the base. Although inaccurate, these measurements showed themes. To choose a location of uniform flow, a location with a high ratio of x-direction velocity to y-direction velocity was desired. Based off of these measurements it was concluded that position 1 showed the best uniform flow among the 8 angles in the tank. Position 1, seen in Figure 13, is the position directly behind the flow straightener.

Once this location was chosen, measurements were collected at all 5 radii, denoted on the board in Figure 14, at this selected position and at positions 10 centimeters further from the flow straightener and 10 centimeters closer to the flow straightener. The idea behind all of these measurements is to create a 3D flow map to compare to the camera particle image analysis to be performed in the future.

Along with all of these 15 data collection points 10 centimeters from the bottom of the tank, 15 positions were collected at two other elevations. One set of measurements at 20 centimeters from the bottom of the tank and the other from 30 centimeters away from the bottom of the tank. These were more accurate and reliable to analyze than the 10 centimeter from base readings, as the sample volume requires 15 centimeters of height, as mentioned before.

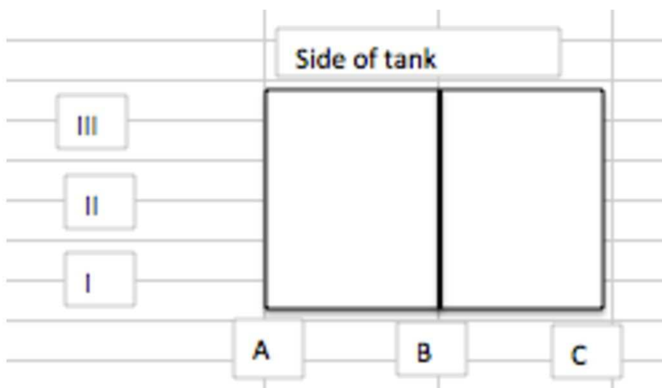

Figure 15: Elevations and distances of readings

Figure 15 shows the notation used for the elevations of the measurements and the distances from the flow straightener. I is 10 centimeters from the base, II is 20 centimeters from the base, and III is 30 centimeters from the base. B is the chosen location from the first round of measurements. A is 10 centimeters further from the flow straightener relative to B and C is 10 centimeters closer to the flow straightener relative to B.

The first round of measurements at the 8 different angles was collected at 32 Hz for 3 minute samples. When the second round of measurements was being collected at the chosen location, technical difficulties ensued causing the sample time to be cut down to about 30 seconds each.

During the data collection, the trolling motor mount slipped due to torque being caused by the motor. This led to the motor's propeller blade slicing a hole in the plastic liner of the tank. Water consequentially began to leak, pictured in Figure 16. To fix the leak, the tank had to be drained out. The tank was drained using the required on-site pump and a siphon created using a garden hose. Once all the water was gone, a patch was placed over the slice in the liner. Time was needed for the adhesive to dry and cure.

Figure 16: Leaks due to sliced hole in liner

The Vector collected velocities of about 0.3 m/s or 30 cm/s. The data of all of the collected velocities can be seen in the appendices.

IV. Tank Sediment Selection

Using the Shields parameter as mentioned before, a sediment size was selected based off of the shear stress and critical Shields parameter for the selected sediment. For this selection, sediment was first chosen as a guess and then analyzed to solve for the Shields parameter. If the Shields parameter is greater than the sediment's critical Shields parameter then it is acceptable to use for this tank experiment because incipient motion will occur. The selected sediment to test if it is expected to see incipient motion in the tank with is sand.

First, the drag coefficient for the tank must be found using Equation 14.

$$C_D = \alpha(\frac{z_o}{h})^\beta \qquad (14)$$

where

$z_o = \frac{d_{50}}{12}$

α = 0.0474, β = 1/3 according to the Manning-Strickler law

Using this equation, the value for bed roughness length, z_0 ,is 0.0167 mm and h, the water depth, is 2 feet, which is about 0.6 meters. Plugging these values into Equation 14, the drag coefficient comes out to be 0.0012.

The drag coefficient can now be used to find the shear stress of the bed, using Equation 15.

$$\tau = \rho \cdot c_D \cdot {U_c}^2 \tag{15}$$

$$\tau = 2650 \cdot 0.0012 \cdot 0.3^2 = 0.289\ [Pa]$$

Knowing that the velocity of sand is 2650 kg/m^3, the drag coefficient just found, and the average tank velocities found using the Vector of about 0.3 m/s, the shear stress of the bed is found to be 0.289 Pa.

This value can be used to find the Shields parameter in Equation 16, which will be compared to the critical Shields parameter for sand, 0.05.

$$\theta = \frac{\tau}{(\rho_s - \rho) g d_{50}} \tag{16}$$

$$\theta = \frac{0.289}{(2650-1000)9.8(0.0002)} = 0.089$$

Dividing the shear stress by the product of the difference of the sand density and water density, gravity, and diameter of the sand, 0.2 mm, gives the Shields parameter for this situation. The Shields parameter is 0.089. The critical Shields parameter for sand is 0.05.

Since the Shields parameter for this scenario is larger than that of the critical Shields parameter, incipient motion is expected to occur and sand is an appropriate choice for the sediment for this experiment.

Conclusions

It can be concluded from the dry experiment using the sand bed test structure consisting of sand from Ogunquit, Maine, that camera imagery analysis is a valid method for measuring incipient motion.

The dry experiment was followed by setting up for performing a similar experiment in water in the circular wave flume in Gregg Hall at the University of New Hampshire. A pressure case for the camera and instrument mounts for the camera, velocimetry sensors, and trolling motor were constructed in preparation.

Velocity measurements were collected using the Vector at multiple angle positions around the tank. An angle close to the flow straightener was chosen as it was characterized by the most uniform flow relative to other tank angles. The velocity measurements were found to be in the range of 30 cm/s.

The velocity measurements collected by the Vector were used to select an appropriately sized sediment grain to put in the tank. It was concluded that using sand in the tank given these velocities would mean the sediment will experience incipient motion, so sand is the chosen sediment. Once the tank is repaired, water will be put back in. Before the sediment is put in the tank, more velocity measurements will be taken with other velocimetry sensors, the Vectrino II and/or Aquadopp as stated previously. More data collection will lead to a more complete flow field measurement to compare to the data that will eventually be collected using the Grasshopper 2 and MatPIV program.

References

Doane, Christopher W. "An Open-Channel Flume for the Study of Two-Dimensional Oil Containment Boom Models in Fast Current." Diss. University of New Hampshire, 1993. Print.

Laursen, Emmett M. "Discussion of "The Legend of A. F. Shields" by Emmett M. Laursen." *Journal of Hydraulic Engineering* 126.9 (2000): 720. Print.

Michel, Claude. "Discussion of "The Legend of A. F. Shields" by Claude Michel." *Journal of Hydraulic Engineering* 126.9 (2000): 721. Print

Rule, John K. "Design Improvements to the University of New Hampshire Ocean Engineering Circulating Water Flume." Diss. University of New Hampshire, 1999. Print.

Soulsby, Richard. *Dynamics of Marine Sands: A Manual for Practical Applications*. London: Telford, 1997. Print.

"Vector." *â ” Nortek AS*. Web. 18 Apr. 2012. <http://www.nortek-as.com/en/products/velocimeters/vector>.

"Welcome to the Point Grey Website. Point Grey Designs, Manufactures and Distributes CCD and CMOS IEEE-1394 (FireWire), USB 2.0, USB 3.0, Gigabit Ethernet (GigE), and Camer Link Cameras. Based in Richmond, BC, Canada, Point Grey Designs, Manufactures and Distributes IEEE-1394 (FireWire) and USB 2.0 Cameras That Are Known for Their Excellent Quality, Performance, and Ease of Use." *Point Grey CCD and CMOS Digital Cameras for Industrial, Machine, and Computer Vision*. Web. 18 Apr. 2012. <http://www.ptgrey.com/>.

Acknowledgements

Dr. Nancy Kinner
Sylvia Rodriguez-Abudo
Meagan Wengrove
Tom Lippman
Charlie Watkins
Nick Tamblyn
Donya Frank
Peter Kinner

Appendices

Grasshopper® 2

POINT GREY
Innovation in Imaging

- Sony progressive scan CCD image sensor, mono or color
- FireWire IEEE 1394b 800 Mbit/s interface
- Compact 44 x 29 x 58 mm case with C-mount lens holder
- Complies with IIDC 1.32

The fully redesigned Grasshopper2 camera series is the next generation version of the high performance Grasshopper. The Grasshopper2 uses the same form factor as the existing Grasshopper, and adds several new features, including enhanced opto-isolated general purpose I/O and improved imaging performance.

IEEE 1394b Models

GS2-FW-14S5M/C-C	1.4 MP	Sony ICX285 CCD, 2/3", 6.45 x 6.45 µm	1384 x 1036 at 30 FPS

FireWire

SPECIFICATIONS	GS2-FW-14S5M / C
Image Sensor Type	Sony progressive scan interline transfer CCD with square pixels and global shutter
Image Sensor Model	Sony ICX285 2/3"
Max Res and Max Frame Rate	1384 x 1036 at 30 FPS
Pixel Size	6.45 x 6.45 µm
Analog-to-Digital Converter	Analog Devices 14-bit ADC
Video Data Output	8, 12, 16 and 24-bit digital data
Image Data Formats	Y8, Y16, Mono8, Mono12, Mono16, Raw16 (all models) RGB, YUV411, YUV422, YUV444, Raw8, Raw12, Raw16 (color model)
Digital Interface	IEEE 1394b 800 Mbit/s interface with screw locks for camera control, data, and power
Partial Image Modes	Pixel binning and region of interest modes available via Format_7
General Purpose I/O Ports	8-pin GPIO connector for power, trigger, strobe, PWM, and serial I/O 1 opto-isolated input, 1 opto-isolated output, 2 bi-directional I/O pins
Gain Control	automatic / manual / one-push gain modes, programmable via software, -3.6dB to 24dB
Shutter Speed	automatic / manual / one-push modes, programmable via software, 0.03ms to 330s (extended shutter mode)
Synchronization	via external trigger, software trigger (on same bus) or free running
External Trigger Modes	External hardware or software trigger Multiple exposure, bulb shutter, multi-shot, and overlapped trigger modes
Voltage / Power	Voltage: 8-30V Power: less than 2.5W
Dimensions (W x H x L)	44mm x 29mm x 58mm (not including lens holder and GPIO connector)
Mass	104 grams (without optics)
Memory Storage	32MB frame buffer, 512 KB non-volatile data flash
Memory Channels	2 memory channels for custom camera settings
Camera Specification	Complies with IIDC 1.32
Lens Mount	C-mount
Emissions Compliance	CE, FCC, RoHS
Operating Temperature	0° to 45°C
Storage Temperature	-30° to 60°C
Vibration Resistance	10 G (14 Hz to 200 Hz)
Status Monitoring	Bi-color LED that can be red, green, or yellow
Warranty	2 Years

North America T +604.242.9937 E sales@ptgrey.com Europe T + 49 7141 488817-0 E eu-sales@ptgrey.com www.ptgrey.com

Fixed Stem Standard

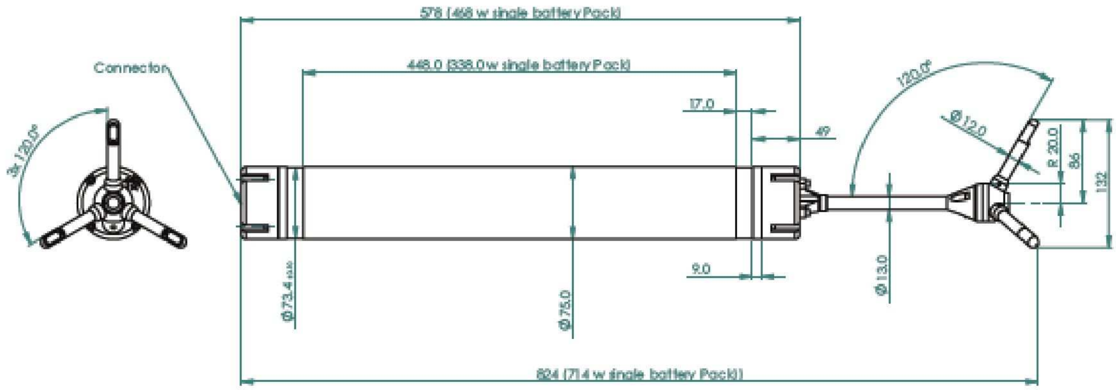

Fixed Stem 4000m

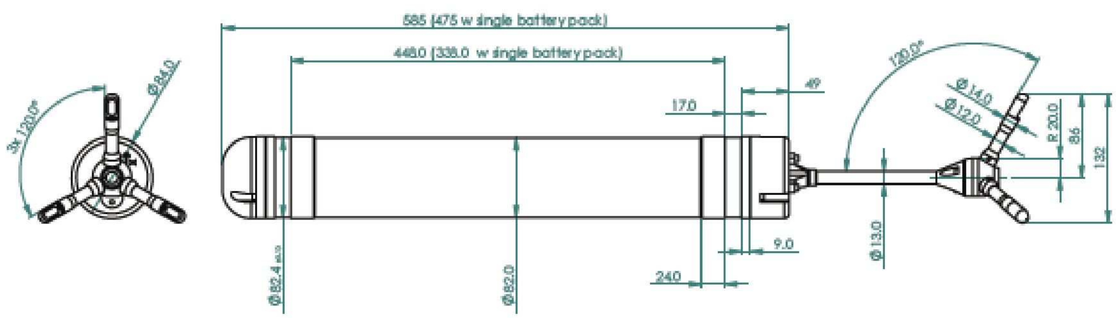

Cable Probe Standard

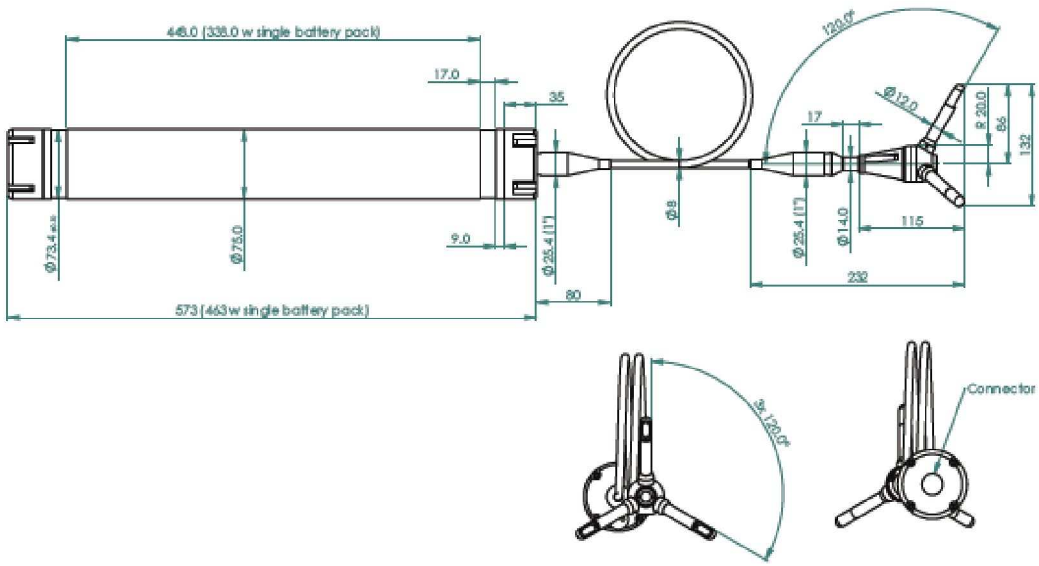

Cable Probe 4000m

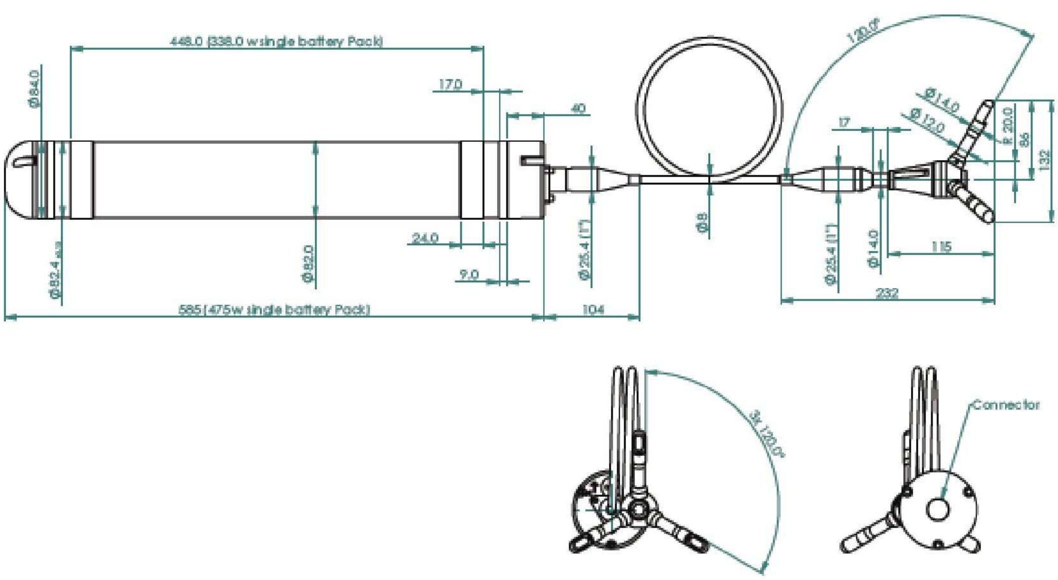

All dimensions in mm.

Technical Specifications

Water Velocity Measurement	
Range:	±0.01, 0.1, 0.3, 2, 4, 7 m/s (software selectable)
Accuracy:	±0.5% of measured value ±1 mm/s
Sampling rate (output):	1–64 Hz
Internal sampling rate:	100–250 Hz
Sampling Volume	
Distance from probe:	0.15 m
Diameter:	15 mm
Height (user selectable):	5–20 mm
Doppler Uncertainty (noise)	
Typ. uncertainty at 16 Hz:	1% of velocity range
Echo Intensity	
Acoustic frequency:	6 MHz
Resolution:	0.45 dB
Dynamic range:	90 dB
Sensors	
Temperature:	Thermistor embedded in end bell
Range:	-4 °C to 40°C
Accuracy/Resolution:	0.1 °C / 0.01°C
Time response:	10 min
Compass:	Magnetometer
Accuracy/Resolution:	2°/0.1° for tilt <20°
Tilt:	Liquid level
Accuracy/Resolution:	0.2°/0.1°
Up or down:	Automatic detect
Maximum tilt:	30°
Pressure:	Piezoresistive
Standard Range:	0–20 m, inquire for options
Accuracy/Resolution:	0.5% / Better than 0.005% of full scale
Data Communication	
I/O:	RS 232 or RS 422. Software supports most commercially available USB– RS 232 converters.
Communication Baud rate:	300–115200
Recorder download baud rate:	600/1200 kBaud for both RS232 and RS422
User control:	Handled via Vector Win32® software, ActiveX® function calls, or direct commands.
Analog outputs:	3 channels standard, one for each velocity component or two velocities and pressure. Output range is 0–5 V, scaling is user selectable.
Analog Inputs	
No. of channels:	2
Supply voltage to analog output devices:	Three options selectable through firmware commands: • Battery voltage/500 mA • +5V/250 mA • +12V/100 mA
Software ("Vector")	
Operating system:	Windows®XP, Windows®7
Functions:	Deployment planning, start with alarm, data retrieval, ASCII conversion. Online data collection and graphical display. Test modes
Data Recording	
Capacity (standard):	9 MB, can add 32/176/352 MB or 4GB (Prolog)
Data record:	24 bytes at sampling rate + 28 bytes/second
Power	
DC Input:	9–15 VDC
Peak current:	3A
Max consumption:	64 Hz 1.5 W
Typ. consumption, 4Hz:	0.6–1.0 W
Sleep consumption:	0.0003 mW (RS232), 0.005 mW (RS422)

Transmitt power:	2 adjustable levels
Battery capacity:	50 Wh
New battery voltage:	13.5 VDC
Data collection capacity:	Refer to planning section in software
Real time clock	
Accuracy:	± 1min/year
Backup in absence of power:	4 weeks
Connectors	
Bulkhead (impulse):	MCBH-8-FS
Cable:	PMCIL-8-MP on 10-m polyurethane cable
Materials	
Standard model:	Delrin® housing. Titanium probe and screws
Environmental	
Operating temperature:	–4°C to +40°C
Storage temperature:	–20°C to +60°C
Shock and vibration:	IEC 721-3-2
Pressure rating:	300 m for canister.
Dimensions	
	see drawings on page 2-3
Weight in air:	5.0 kg (standard), 8.3 kg (4000m)
Weight in water:	1.5 kg (standard), 5.1 kg (4000m)
Options	
Acoustic beams:	Probe mounted on fixed stem or on 2-m cable (see drawing)
Batteries:	Lithium or Lithium Ion
External batteries:	Alkaline, Lithium or Lithium Ion (see battery brochure for details)
Pressure sensor:	Specify range.

In most cases, the Vector is deployed as a self contained instrument with internal recorder, or connected to an on-line PC. It can also be operated from any third-party controller using RS 232 or RS 422 communication.

NortekMed S.A.S.
Z.I. Toulon Est
BP 520
83 078 TOULON cedex 09
FRANCE
Tel: +33 (0) 4 94 31 70 30
Fax: +33 (0) 4 94 31 25 49
E-mail: info@nortekmed.com

NortekUK
Mildmay House, High St.
Hartley Wintney
Hants. RG27 8NY
Tel: +44-1428 751 953
E-mail: inquiry@nortekuk.co.uk

NortekUSA
222 Severn Avenue
Building 14, Suite 102
Annapolis, MD 21403
Tel: +1 (410) 295-3733
Fax: +1 (410) 295-2918
E-mail: inquiry@nortekusa.com

[illegible]
Tel: 0532-85017570, 85017270
Fax: 0532-85017570
E-mail: inquiry@nortek.com.cn

Nortek B.V.
Schipholweg 333a
1171PL Badhoevedorp
Nederland
Tel: +31 20 6543600
Fax: +31 20 6599830
email: info@nortek-bv.nl

Flow Field Measurments
15-Apr-12

Choosing Location

Ben Anibal
Laura Baldinger
Dustin Metayer

Velocities [m/s]

1 - middle of the board

Angles	x	y	z	x/y
1	-0.0017	0.0004	-0.0002	**-4.25**
2	-0.0158	-0.0575	0.0111	**0.27**
3	-0.0005	-0.0002	-0.0003	**2.50**
4	0.0023	0.003	-0.0003	**0.77**
5	-0.0015	0.001	0.0002	**-1.50**
6	-0.0001	-0.0007	-0.0002	**0.14**
7	0.0014	-0.0028	-0.0003	**-0.50**
8	-0.0005	-0.0023	0	**0.22**

Note: ruled out angle positions 4 through 8 because of low x/y ratios

2 - 6.5" away from outer edge of tank

Angles	x	y	z	x/y
1	-0.0047	0.0075	-0.0016	**-0.63**
2	-0.0237	0.038	0.0053	**-0.62**
3	0.0013	0.0007	-0.0003	**1.86**

3 - 9" away from outer edge of tank

Angles	x	y	z	x/y
1	0.0107	0.0045	0.0001	**2.38**
2	-0.0037	0.0064	0.0053	**-0.58**
3	-0.0002	-0.0029	-0.0009	**0.07**

4 - 9" away from inner edge of tank

Angles	x	y	z	x/y
1	-0.001	0.0041	0.0001	**-0.24**
2	-0.0022	-0.0079	-0.0006	**0.28**
3	-0.0015	-0.0004	0.0002	**3.75**

5 - 6.5" away from inner edge of tank

Angles	x	y	z	x/y
1	0.0151	-0.0247	-0.0042	**-0.61**
2	-0.0005	-0.0012	-0.0002	**0.42**
3	-0.0029	0.0041	0.0007	**-0.71**

Board hole notation

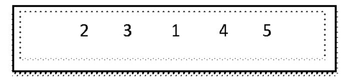

Tank angle notation

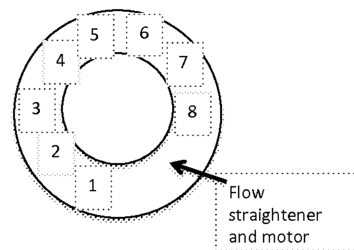

Note: 3 minute samples were taken for each at a sampling rate of 32 Hz
Vector was used to take measurements 10 cm from the base of the tank

All of these measurements were taken at a height of 10 cm from bottom of tank

Data collected when trolling motor was set to level 3 (half of its maximum)

17-Apr-12

Map of Chosen Location

Ben Anibal
Laura Baldinger
Dustin Metayer

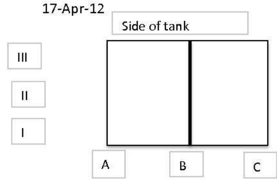

Note: This is a diagram of the side of the tank looking in. The chosen distance from the flow straightener was Angle 1 from the previous tab. B represents Angle 1. A is 10 centimeters farther away from the flow straightener relative to B and C is 10 centimeters close to the flow straightener relative to

Note: Measurements were taken at three distances from the flow straightener and 3 elevations to complete a 3D flow map of the chosen location. I is 10 centimeters above the base of the tank, II is 20 cetimeters from the base of the tank and III is 30 centimeters from the base of the tank.

Board hole notation

2	3	1	4	5

Note: Samples taken at 32 Hz for a sampling time of about a minute for each. Sampling time was cut down from previous measurements due to a leak in the tank caused by the propellor blade slicing the tank liner.

Velocities [m/s]

Data collected when trolling motor was set to level 3 (half of its maximum)

1 - middle of the board

	A - 10 cm further from flow straightener than chosen position				B - chosen position				C - 10 cm closer to flow straightener than chosen position			
Height	x	y	z	**x/y**	x	y	z	**x/y**	x	y	z	**x/y**
I (10 cm from base)	0.0019	-0.0047	-0.004	**-0.40**	-0.0017	0.0004	-0.0002	**-4.25**	0.0017	0.0041	-0.0006	**0.41**
II (20 cm from base)	-0.3031	0.0605	0.0246	**-5.01**	-0.2171	0.1775	-0.0727	**-1.22**	-0.2294	0.1225	-0.0463	**-1.87**
III (30 cm from base)	-0.3734	0.143	-0.0666	**-2.61**	-0.3171	0.0669	-0.022	**-4.74**	-0.3951	0.0723	-0.0159	**-5.46**

2 - 6.5" away from outer edge of tank

	A - 10 cm further from flow straightener than chosen position				B - chosen position				C - 10 cm closer to flow straightener than chosen position			
Height	x	y	z	**x/y**	x	y	z	**x/y**	x	y	z	**x/y**
I (10 cm from base)	0.0137	0.0065	-0.0003	**2.11**	-0.0047	0.0075	-0.0016	**-4.25**	0.0116	-0.0033	0.0013	**-3.52**
II (20 cm from base)	-0.2357	0.1292	-0.0571	**-1.82**	-0.2627	0.1218	-0.0377	**0.27**	-0.2662	0.1073	-0.051	**-2.48**
III (30 cm from base)	-0.2382	0.0844	-0.0275	**-2.82**	-0.2808	0.1121	-0.0572	**2.50**	-0.2925	0.1071	-0.0362	**-2.73**

3 - 9" away from outer edge of tank

	A - 10 cm further from flow straightener than chosen position				B - chosen position				C - 10 cm closer to flow straightener than chosen position			
Height	x	y	z	**x/y**	x	y	z	**x/y**	x	y	z	**x/y**
I (10 cm from base)	0.0099	-0.0052	0.0004	**-4.25**	0.0107	0.0045	0.0001	**-4.25**	0.0066	0.0025	0.0012	**2.64**
II (20 cm from base)	-0.0827	0.1496	-0.0989	**0.27**	-0.2131	0.1538	-0.0781	**0.27**	-0.2578	0.0952	-0.0257	**-2.71**
III (30 cm from base)	-0.258	0.0995	-0.0744	**2.50**	-0.2536	0.0704	-0.0481	**2.50**	-0.3047	0.1125	-0.0352	**-2.71**

4 - 9" away from inner edge of tank

	A - 10 cm further from flow straightener than chosen position				B - chosen position				C - 10 cm closer to flow straightener than chosen position			
Height	x	y	z	**x/y**	x	y	z	**x/y**	x	y	z	**x/y**
I (10 cm from base)	-0.0044	0.0016	-0.0003	**-4.25**	-0.001	0.0041	0.0001	**-4.25**	-0.0003	0.0044	0.0012	**-0.07**
II (20 cm from base)	-0.3821	0.1297	-0.0351	**0.27**	-0.332	0.1247	-0.0386	**0.27**	-0.2853	0.1041	-0.0371	**-2.74**
III (30 cm from base)	0.262	-0.0739	0.0795	**2.50**	0.2941	0.097	0.0548	**2.50**	0.0872	0.1263	0.0712	**0.69**

5 - 6.5" away from inner edge of tank

	A - 10 cm further from flow straightener than chosen position				B - chosen position				C - 10 cm closer to flow straightener than chosen position			
Height	x	y	z	**x/y**	x	y	z	**x/y**	x	y	z	**x/y**
I (10 cm from base)	-0.0057	0.0032	-0.0004	**-4.25**	0.0151	-0.0247	-0.0042	**-4.25**	0.0012	0.0006	-0.005	**2.00**
II (20 cm from base)	-0.3555	0.0611	0.0042	**0.27**	-0.3129	0.099	-0.0088	**0.27**	-0.3133	0.093	-0.0418	**-3.37**
III (30 cm from base)	-0.1795	-0.0129	0.0073	**2.50**	0.1324	0.1548	0.0914	**2.50**	0.0854	0.1609	-0.0123	**0.53**